Factors governing Mass Transfer during the Regeneration of LiCl solution as a Liquid Desiccant by Electrodialysis

Ali Al-Jubainawi[1,*], Zhenjun Ma[1], Yi Guo[1], Long D. Nghiem[2], Paul Cooper[1], Weihua Li[3]

[1]Sustainable Buildings Research Centre, University of Wollongong,

Wollongong, NSW, 2500, Australia

[2]School of Civil, Mining & Environmental Engineering, University of Wollongong

[3]School of Mechanical, Materials & Mechatronic Engineering, University of Wollongong

*E-mail:ahjaj349@uowmail.edu.au.

ABSTRACT: This study investigates the mass transfer and performance of electrodialysis (ED) for LiCl liquid desiccant regeneration for air conditioning and dehumidification. Experiments were conducted using an ED system with ten cell pairs of ion-exchange membranes. Numerical simulation using Nernst-Plank equations and computational fluid dynamic technique was performed using COMSOL Mulphysics and the results were validated using experimental data. The results showed that the water flux due to osmosis and electro-osmosis during ED regeneration of LiCl liquid desiccant was significant and could not be ignored unlike most other desalination applications. The water flux due osmosis and electro-osmosis are directly associated with the osmotic gradient and applied current between the cathode and anode, respectively. On the other hand, the salt flux due osmosis was insignificant. The model used in this study was validated using experimental data. Simulation was then conducted to elucidate the relationship between concentration profile of LiCl along the membrane surface and concentration polarisation in the ED channel with respect to circulation flow rate, applied current, and cell width. Overall, the results suggest that concentration difference between the regenerated and spent LiCl should be minimised for an optimum ED performance.

Keywords: Liquid desiccant; Mass transfer mechanism; Electrodialysis; Experimental investigation; Numerical simulation

Nomenclature

A_{cell}	Membrane surface area (m^2)
B	Membrane water permeability due to the osmotic pressure difference between both sides of the membrane ($mol.m^{-2}.sec^{-1}.bar^{-1}$)
C	Weight per weight concentration [% (wt/wt)] or molar concentration ($mol.m^{-3}$)
C_{ED}	Weight per weight concentration from spent to regenerated channels (%)
D	Diffusion coefficient ($m^2.sec^{-1}$)
F	Faraday's constant (96485 $C.mol^{-1}$)
I	Current intensity (A)
i	Current density ($A.m^{-2}$)
J	Molar flux ($mol.m^{-3}$)
L	Channel length (m)
M_{H_2O}	Water molecules (g/mol)
m	Mass ($g/s.m^2$)
N	Number of cells (-)
n	Mole number
R	Universal gas constant 0.08314 (L bar K^{-1} mol^{-1})
T	Temperature (K)
t	Time (sec)
t_w	Water transport number (-)
u	Ions mobility ($m^2 .s^{-1} .volt^{-1}$)
V	Volume (m^3)
$\dot{V}$	Volumetric flow rate ($m^3.sec^{-1}$)
v	Velocity ($m.sec^{-1}$)
W	Width (m)
W_m	Membrane thickness (m)
z	valance of anions (-)
Greek symbols	
σ	Electrical conductivity of the membrane ($S.m^{-1}$)
∅	Applied voltage (volt)
π	Osmotic pressure (bar)
ρ	LiCl solution density (kg. m^{-3})
Superscript	
i	Initial condition
t	Time step
Subscript	
AEM	Anionic exchange membrane
CEM	Cationic exchange membrane
GT	Regenerated tank
Cl	Chlorine
Ch	Channel

G	Regenerated compartment
S	Spent compartment
ST	Spent tank
Dif	Diffusion
Eos	Electro-osmosis
In	Inlet
I	Due to applied current
Li	Lithium
LiCl	Lithium chloride
M	Membrane
Os	Osmosis
S	Specie and solution
tot	Total
W	Water
$\pm$	Negative or positive charge

1. Introduction

The increase in energy demand for air conditioning and climate changes are some of the most significant challenges facing the building sector [1]. The building sector accounts for around 40% of total world energy usage, of which about 50% is attributed to heating, ventilation and air conditioning (HVAC) [2, 3]. Building energy efficiency is therefore essential to reduce global energy usage and greenhouse gas emission.

Over the last few decades, several energy-efficient technologies have been proposed for improving the performance of building HVAC systems [4-6]. Among them, desiccant cooling has emerged as an attractive approach [7, 8]. Desiccants are hygroscopic or dehumidified substances with the ability to attract moisture from air based on their affinity to water [7, 9]. To maintain the dehumidification capability, it is necessary to continuously regenerate the desiccants to remove water molecules [10].

Regeneration of liquid desiccants is therefore a key process in a desiccant cooling system. Solar thermal regeneration is a common technique since solar energy availability usually coincides with high demand for desiccant cooling [11]. Nevertheless, the high temperature of liquid desiccants after the regeneration process can impede the overall performance of desiccant

cooling systems. Therefore, several non-thermal regeneration techniques have also been studied. Al-Sulaiman *et al.* [12] proposed a liquid desiccant cooling system using a reverse osmosis (RO) process for regeneration. However, a high pressure pump was required to overcome the high osmotic pressure of the liquid desiccant [12]. Another approach is to use the electrodialysis (ED) process to regenerate liquid desiccants [13]. ED is an ion-exchange membrane separation process. In ED, ions can be transported through selective cation or anion membranes under an electric potential gradient [14]. Owing to the selectivity of ion-exchange membranes, cations and anions can only migrate through cation-exchange membranes (CEMs) and anion-exchange membranes (AEMs), respectively.

ED application for liquid desiccant regeneration was first proposed by Li and Zhang [13], who used a single stage photovoltaic-electrodialysis (PV-ED). A double stage PV-ED system was subsequently developed by Li *et al.* [15] leading to 50% energy saving in comparison to their first single stage PV-ED system. Cheng *et al.* [16] developed a hybrid ED regeneration system, in which the heat regenerated by solar photovoltaic thermal collectors was used to pre-treat the liquid desiccant solution before entering the ED stack. The results from these studies have demonstrated the practicality of ED technology for liquid desiccant regeneration. However, the remaining technical challenge is to determine the operational envelop and optimise ED operation specifically for liquid desiccant regeneration.

Mass transfer of ions and water ion-exchange membranes has been extensively investigated both theoretically and experimentally [17-25]. However, most if not all of these previous studies were in the context of sea or brackish water desalination in which salt concentrations in the feed were much lower than that used for liquid desiccant regeneration. Tanaka [17] developed an experimental and theoretical procedure to investigate the mass transport and energy consumption of ED for seawater desalination. Nikonenko *et al.* [18] proposed a model which considered two chemical species in the external diffusion boundary. The mechanism of the

competitive transport of anions through AEMs was described using the Nernst-Plank and Donnan equations [18]. A mathematical model based on the Nernst-Plank equation was also used by Casas *et al.* [19, 20] to predict the performance of an ED system for reconcentrating the brine of the reverse osmosis of the seawater desalination process.

To date, there have been very few attempts to model and optimise the performance of ED specifically for liquid desiccant regeneration. An experimental setup was developed by Cheng *et al.* [26] to examine the effect of the solution flow rate on the mass transfer and current utilization of the ED stack. Guo *et al* [27] experimentally investigated the effects of four operating parameters of ED on the concentration increase of the liquid desiccant solution. The four operating parameters considered were the initial concentration of the regenerated solution, the initial concentration difference between the regenerated and spent solutions, the applied current density and the solution flow rate. The results from the experimental tests showed that ED technology can be potentially used for LiCl liquid desiccant regeneration if the operating conditions of ED are properly selected.

A key distinction between ED for desalination and liquid desiccant regeneration is the mass transfer induced by osmotic, electro-osmotic, ion migration, and diffusion. This study aims to elucidate the mass transfer mechanisms of ED for regenerating lithium chloride liquid desiccant commonly used in desiccant cooling systems through both numerical simulation and experimental evaluation.

2. Theory

2.1 Mass transfer mechanisms

There are four major mass transfer mechanisms in ED namely electro-osmosis, osmosis, ion migration and diffusion. Electro-osmosis and osmosis are responsible for water transport. Ion migration and diffusion govern the transport of ions through the membrane. Osmosis occurs when there is a difference between the spent and regenerated solution concentrations across the

membrane. Osmosis leads to the transfer of water from the spent solution (low osmotic pressure) to the regenerated solution (high osmotic pressure) and the salt diffusion in the opposite direction [14]. Salt diffusion through selective membranes is generally small compared to that governed by ion migration, which is induced by an applied electrical potential between the cathode and anode in the ED stack [25, 28]. Because of hydration, each ionic in an aqueous solution is surrounded by a thin layer of the water molecules [14]. These water molecules will transport together with the migrated ions due to the electro-osmosis phenomena [28]. Thus, the concentration and the volume in the regenerated channels gradually increase due to the ions migration and water transfer when an electric current is applied to the ED stack.

2.2 Data analysis methods

A total of 21 experiments (Table 1) were conducted using a lab-scale ED system. Experimental data were used to investigate the water and salt fluxes due to the applied electrical current, the diffusion, different osmotic pressures and the electro-osmosis impacts. The water flux ($\Delta m_{w,os}$) and salt flux ($\Delta m_{salt,Dif}$) through the ED channels due to osmosis and diffusion without current apply can be determined using Eqs. (1) and (2), respectively.

$$\Delta m_{w,os}^{i+t} = \frac{1}{2N.A_{cell}.t}.\left[\rho_{GT}^{i+t}.V_{GT}^{i+t}\left(1-C_{GT}^{i+t}\right)-\rho_{GT}^{i}.V_{GT}^{i}\left(1-C_{GT}^{i}\right)\right] \quad (1)$$

$$\Delta m_{salt,Dif}^{i+t} = \frac{1}{2N.A_{cell}.t}.\left[\rho_{ST}^{i+t}.V_{ST}^{i+t}.C_{ST}^{i+t}-\rho_{ST}^{i}.V_{ST}^{i}.C_{ST}^{i}\right] \quad (2)$$

When an electric current is applied, both osmosis and electro-osmosis can affect the water flux from the spent channels to the regenerated channels and the total water flux ($\Delta m_{w,tot}$) can be determined by Eq. (3).

$$\Delta m_{w,tot}^{i+t} = \Delta m_{w,os}^{i+t} + \Delta m_{w,eos}^{i+t} = \frac{1}{2N.A_{cell}.t}.\left[\rho_{GT}^{i+t}.V_{GT}^{i+t}\left(1-C_{GT}^{i+t}\right)-\rho_{GT}^{i}.V_{GT}^{i}\left(1-C_{GT}^{i}\right)\right] \quad (3)$$

The net salt mass flux ($\Delta m_{salt,net}$) through the ED membranes with applied current is a combination of the effects of the ions migration and diffusion and can be calculated by Eq. (4).

The mass flux from the spent channels to the regenerated channels of the ED stack (Δm_{ED}) can therefore be determined by Eq. (5).

$$\Delta m_{salt,net}^{i+t} = \Delta m_{salt,I}^{i+t} - \Delta m_{salt,Dif}^{i+t} = \frac{1}{2N.A_{cell}.t}.\left[\rho_{GT}^{i+t}.V_{GT}^{i+t}.C_{GT}^{i+t} - \rho_{GT}^{i}.V_{GT}^{i}.C_{GT}^{i}\right] \quad (4)$$

$$\Delta m_{ED}^{i+t} = \Delta m_{w,tot}^{i+t} + \Delta m_{salt,net}^{i+t} \quad (5)$$

where, $\Delta m_{salt,I}$ is the salt mass transfer due to applied current, and C, ρ, t, N, A_{cell} and V are the concentration, density, operating time, cells number, effective membrane area and volume of the solution respectively, the superscribes $i+t$ and i represent the time since the start of the test and the start time of the test respectively, and the subscribes GT and ST indicate the regenerated and spent tanks, respectively.

The concentration of the solution transferred from the spent channels to the regenerated channels C_{ED} can be determined by Eq. (6), which can provide an indication on the ED regeneration performance under different operating conditions.

$$C_{ED}^{i+t} = \frac{\Delta m_{salt,net}^{i+t}}{\Delta m_{w,tot}^{i+t} + \Delta m_{salt,net}^{i+t}} \quad (6)$$

Because of ion and water transport, the concentration and volume in both generated and spent tanks vary with the time. These changes can be calculated using the mass balance equation for both spent and regenerated tanks. Therefore, the concentrations of the spent and regenerated solutions at the exit of the ED stack can be determined by Eqs. (7) and (8), respectively.

$$C_{2}^{i+t} = \frac{C_{GT}^{i+t}.\rho_{GT}^{i+t}.\dot{V}_1 + \Delta m_{ED}^{i+t}.C_{ED}^{i+t}}{\rho_{GT}^{i+t}.\dot{V}_1 + \Delta m_{ED}^{i+t}} \quad (7)$$

$$C_{4}^{i+t} = \frac{C_{ST}^{i+t}.\rho_{ST}^{i+t}.\dot{V}_2 - \Delta m_{ED}^{i+t}.C_{ED}^{i+t}}{\rho_{ST}^{i+t}.\dot{V}_2 - \Delta m_{ED}^{i+t}} \quad (8)$$

where, C_2 and C_4 are the concentrations of the solutions at the exits of the regenerated channels and spent channels respectively, and $\dot{V}_1$ and $\dot{V}_2$ are the volumetric flow rates of the solutions in the regenerated and spent cycles, respectively.

2.3 Numerical modelling of the ED cell

A concurrent ED cell consisting of one regenerated domain, two spent domains, and one pair of cation and anion exchange membranes was modelled in this study (Fig. 1). The geometric dimensions of the ED cell were specified based on the manufacturing catalogue of the experiment rig. Key parameters used in the model are summarised in Table 2.

The Nernst-Plank equation has been extensively used to simulate the ions transport through ED membranes [19, 25, 28, 29] and this equation has been included in the electrochemistry component of COMSOL Multiphysics Software. COMSOL Multiphysics is a commercial finite element package designed to address a wide range of physical phenomena [30]. The procedures to simulate ED for liquid desiccant regeneration using COMSOL Multiphysics are available in detail elsewhere [25, 31].

The Nernst-Plank equation for the diffusion, migration and convection, used to simulate the ions movement behaviour inside the ED cells is shown in Eq. (9):

$$J_s = -D_s \nabla c_s - z_s u_s F c_s \nabla \emptyset + c_s v \quad (9)$$

where, J and c stand for the molar flux and the concentration respectively, D is the diffusion coefficient, z is the charge number of ions, u is the mobility, F is the Faraday constant, ϕ is the solution potential, v is the fluid velocity vector, and the subscript s represents the kind of species such as cations and anions.

For liquid desiccant regeneration, the product from the ED stack is the regenerated solution with a high concentration and the performance of the ED regeneration can be affected by the amount of water transferred from the spent channels to the regenerated channels. Therefore, the water flux through the selective membranes due to the osmosis and electro-osmosis has to be considered and is calculated using Eqs. (10) and (11), respectively [28], in which the water transport number due to the electro-osmosis and water permeability factor of the membranes due to osmosis were obtained from the experiments.

$$\dot{m}_{w,os} = B.\,n.\,R.\,T.\,M_{H_2O}\,(c_G - c_S) \tag{10}$$

$$\dot{m}_{w,eos} = \frac{t_w i}{F} \times M_{H_2O} \tag{11}$$

where, $\dot{m}_{w,os}$ and $\dot{m}_{w,eos}$ are the water flux from the spent to the regenerated channels due to osmosis and electro-osmosis impacts respectively, B is the water permeability factor of AEMs and CEMs, M_{H_2O} is the weight molecules of water, n is the moles number of the solute in the solution, R is the gas constant, T is the absolute solution temperature, i is the applied current density, t_w is the water transport number of membranes, and the subscribes G and S represent the regenerated and spent channels, respectively.

The heat transfer between the spent and regenerated channels of the ED cells was not considered in this study. In addition, it was assumed that the regenerated and spent channels have the same hydrodynamic characteristics as the same solution flow rates were used in both flow channels.

2.4 Boundary conditions

The major boundary conditions of the ED stack used for liquid desiccant regeneration were similar to those presented in Zourmand *et al.* [25]. They are schematically illustrated in Fig 1 and are briefly summarised below:

- The potential drop (i.e. ∅) across the ED cell is constant;
- The concentrations of the spent and regenerated solutions at the ED entrance are uniform, respectively;
- The gradient diffusion flux at the exit of the ED channels equals to zero;
- The current density of the solution equals to the current density of the membrane; and
- Anionic ions can only pass through the AEM and cationic ions can only transfer through the CEM.

3. Materials and Methods

3.1 Electrodialysis system

A lab-scale ED system (Fig. 2) consisting of an ED stack, a rectifier (PowerTech MP3090) and a power transformer was used. Key specifications of the ED stack (Asahi Glass Corp., Tokyo, Japan) are summarised in Table 3. Lithium sulphate (Li_2SO_4) solution was used as the electrode rinsing solution in the ED stack. Two extra cation CMV membranes were used at the cathode and anode to prevent sulphate from migrating into the spent and regenerated solutions. The regenerated, spent and electrolyte solutions were circulated through three 3.5 L Perspex tanks, respectively. The solutions were circulated through the ED stack by three magnetic drive pumps. Further details of this ED system are available elsewhere [27].

A portable density meter (30PX Densito) was used to measure the density and temperature of the aqueous LiCl solutions in both regenerated and spent tanks. The measured density and temperature were then used to calculate the concentrations of the LiCl solutions. Three direct indication type variable area flow meters with a scale range of 60-600 L/h were used to measure the solution flow rates in each individual flow stream.

3.2 Experimental protocol

Four sets of the experiments (Table 1) were conducted to investigate the mass transfer mechanisms and the impact of the solution flow rate and applied current on the performance of ED for liquid desiccant regeneration. The density and temperature of the solutions in both spent and regenerated tanks were measured every 5 minutes.

The first experimental set examined the water transfer through the membranes resulting from the osmotic pressure difference due to the different solution concentrations between the spent and regenerated channels, and to investigate the salt transfer from the regenerated channel to the spent channel due to diffusion.

The second experimental set investigated the water transfer through the selective membranes due to the electro-osmotic impact when different currents were applied to the ED stack. Each

experiment was carried out with the same initial concentrations in both the spent and generated tanks and the same solution flow rate.

The third experimental set was designed using Taguchi method with orthogonal arrays for four factors and three levels. This set of experiment was to examine the salt mass transfer through the members with different combinations among the applied electrical current, solution flow rate, and the initial concentrations of the solutions in the spent and generated tanks.

The last experimental set examined the effects of the solution flow rate on the performance of the ED for liquid desiccant regeneration. The experiments were performed with three different solution flow rates under the same applied current of 8 A. The initial concentrations of the solutions in both spent and regenerated tanks were almost the same and were around 27.5% (wt/wt).

4 Results and discussion

4.1 Model validation

To ensure the Nernst-Plank model validity for liquid desiccant regeneration, the results obtained using COMSOL Multiphysics were validated using the data collected from the third experiment set (Fig. 3). The simulated concentration difference of the solution at the entrance and exit of the regenerated channels was in good agreement with experimental data. The results in Fig. 3 confirm that the Nernst-Plank model integrated with COMSOL Multiphysics can provide acceptable estimates for predicting the concentration of the solution at the ED outlet.

4.2 *Water and salt transfer* due to osmosis

Fig. 4 shows the osmotic pressure differences between the spent and regenerated channels as well as the transfer of water and LiCl through the membranes at various concentration differences between the two solutions (i.e. experimental cases 1-5). There was no electrical potential between the cathode and anode to eliminate any electro-osmosis effect. The circulation flow rate was 100 L/h.

The osmotic pressure difference between the spent and regenerated channels decreased with time since the concentration difference between both channels also decreased continuously over time (Fig. 4a). With increasing osmotic pressure differences between the spent and regenerated channels, the amount of water transferred from the spent channels to the regenerated channels increased with the operation time (Fig. 4b). The maximum water transfer from the spent to the regenerated tanks within 2 hours operation was about 0.28 g/s.m^2 when the initial concentration difference between the spent and regenerated solutions was 25% (wt/wt), whereas the transfer of water decreased to 0.018 g/s.m^2 when the initial concentration difference between the spent and regenerated solutions decreased to 5% (wt/wt).

Salt diffusion due to the concentration difference between the spent and regenerated channels was generally small when comparing to that of water transfer (Fig. 4c). The highest salt flux was 0.09 g/s.m^2 when the initial concentration difference of the solutions between the spent and regenerated channels was 25%.

Overall, water transport due to osmosis is more significant than salt transport. It is necessary to minimise the concentration difference between the spent and regenerated solutions to control the negative impact of osmosis on ED performance for liquid desiccant regeneration.

4.3 Water transfer due to electro-osmosis

In this study, four experiments (i.e. test cases of 6-9) were carried out to investigate the impact of the electro-osmosis on the amount of water transfer from the spent channels to the regenerated channels. Concentration of the spent and regenerated channels was identical to avoid any osmosis effect.

Fig. 5 shows the transfer of water from the spent to the regenerated channels under different applied currents. The transfer of water increased with the increase of the applied current. When the initial concentrations of the solutions in both spent and regenerated tanks were 30% (wt/wt) and the solution flow rate of 100 L/h, the amount of water flux was about 0.170 and 0.041

g/s.m^2 when the applied currents were 12 and 3 A, respectively (Fig. 5a). When the initial concentrations of the solutions in both spent and regenerated tanks were 18% (wt/wt), the amount of water transferred from the spent solution to the regenerated solution increased to 0.290 and 0.071 g/s.m^2 when the applied currents were 12 and 3 A, respectively (Fig. 5b). Thus, the transfer of water through the membranes decreased with increasing salt concentration. This phenomenon could be resulted from high water activity in low solution concentration and obstruction of the boundary layers for mass transfer through ion exchange membranes, where an increased solution concentration led to an increased solution viscosity thereby increasing the boundary layer thicknesses at the membrane walls [32].

4.4 Ion transfer due to applied current

The salt transfer during ED was analysed using the third experiment set (i.e. test cases 10-18). Table 4 summarises the salt transfer from the spent to the regenerated tanks within 1 hour test under different operating conditions. Salt transfer can be generally classified into three groups (i.e. 0.048-0.054, 0.062-0.071, and 0.082-0.079 g/s.m^2) corresponding to the applied currents of 8, 10, and 12 A, respectively. The applied current is the most influential parameter for the salt transfer through the membranes. Increasing the applied current increased the salt transfer from the spent to the regenerated channels regardless of the solution flow rate and the initial solution concentrations of the solutions in both spent and regenerated tanks.

The performance of ED for the liquid desiccant regeneration was also evaluated based on the concentration difference of the regenerated solution between the entrance and the exit of the ED stack. As shown in Table 4, the concentration difference of the regenerated solution between the entrance and the exit of the ED stack decreased with increasing initial concentration difference of the solutions between the spent and regenerated tanks. This was primarily due to the increasing osmotic pressure difference between the spent and the regenerated channels

thereby deteriorating the ED regeneration performance. Under the same applied current, the amount of the salt transfer from the spent tank to the regenerated tank was very close when changing the solution flow rate.

The impact of the solution flow rate on the ED regeneration performance was investigated based on the experimental data from the test cases of 19-21(Fig. 6). As expected, the concentration difference of LiCl between the entrance and the exit of the ED stack increased with the decrease of the solution flow rate due to the increasing residential time of the solution inside the ED stack.

4.5 Concentration profile of LiCl in the ED channels

The concentration profile of LiCl along the ED cell with different solution flow rates was simulated under the applied current of 8 A and the initial concentrations of both spent and regenerated solutions of around 29.031% (wt/wt) and the results are presented in Fig. 7. Concentration of the regenerated solution continuously increased along the length of the membranes and the concentration of the solution at the ED exit increased with the decrease of the solution flow rate. The concentration difference of the solution between the entrance and exit of the regenerated channels was 0.053% (wt/wt) when the applied current was 8 A, the concentrations of both spent and regenerated solutions at the ED entrance were 29.031% (wt/wt), and the solution flow rate was 20 L/h. The concentration difference of the solution between the entrance and exit of the regenerated channel decreased to 0.0077% (wt/wt) when the solution flow rate was increased to 140 L/h while keeping the other operating conditions were the same. The above results showed that decreasing the solution flow rate between ED cell membranes can greatly improve the performance of ED for liquid desiccant regeneration.

Fig. 8 shows the simulated concentration profile of LiCl at the exit and the entrance of the ED cells under different solution flow rates (60, 100 and 140 L/h) and the applied current of 8 A and the concentrations of both spent and regenerated solutions at the ED entrance of 29.031%

(wt/wt). In the regenerated channel, the concentration of the bulk solution was always lower than that at the membrane walls, while the concentration of the bulk solution in the spent channels was higher than that at the membrane walls (Fig. 8).

Fig. 8 also shows a thin boundary layer at the ED entrance while the thickness of this boundary layer increased gradually along the membrane walls in the regenerated side of the ED channels. A significant boundary layer can be observed at the exit of the ED cell and the thickness of the boundary layer increased when decreasing the solution flow rate from 140 to 100 and 60 L/h, as shown in Fig. 8b-d, respectively.

Fig. 9 illustrates the concentration polarisation profile along the length of the CEM and AEM when the concentrations of the solutions at the entrance of both spent and regenerated channels were 29.031% (wt/wt), and the solution flow rate was 60 L/h. The thickness of the boundary layers on the CEM was larger than that on the AEM and this was because the mobility of Cl^- ions was larger than that of Li^+ ions [14]. As a result, in the regenerated channel, the concentration on the AEM surface was less than that on the CEM surface. The concentration at the membrane walls increased with the increase of the applied current. However, in the spent channel, the concentration at the membrane wall decreased with the increase of the applied current. The maximum concentration at the CEM wall in the regenerated channel was about 29.9% (wt/wt), while the minimum concentration at the same membrane wall in the spent channel decreased to 28.1% (wt/wt) when the applied current was 12A.

4.6 Flux of ions through membranes

Fig. 10 shows a comparison between the fluxes of Li^+ and Cl^- ions in the bulk solution when the current applied varied from 3 to 12 A under the same concentrations of both spent and regenerated solutions at the ED entrance of 29.031% (wt/wt) and the solution flow rate of 60L/h. The fluxes of Li^+ and Cl^- ions became dominant around the CEM and AEM of the ED cell, respectively. When the applied current was 12 A, the flux of Li^+ ions was 0.014 g/sec.m^2

towards the CEM in the boundary layer and the flux of Cl^- ions was 0.07 g/sec.m^2 towards the AEM in the boundary layer. However, when the applied current was 3A, the fluxes of Li^+ and Cl^- ions were 0.003 and 0.017 g/s.m^2 towards the CEM and AEM in the boundary layer, respectively. Therefore, salt transfer from the spent to the regenerated channels in the ED cell was strongly affected by the current applied.

Fig. 11 presents a comparison between the total salt fluxes transferred into the regenerated channels derived based on the experimental data and that determined based on the simulation data under different applied currents and the same concentration of both spent and regenerated solutions at the ED entrance of 29.031% (wt/wt) and the solution flow rate of 60 L/h. It is shown that the total salt flux transferred through the membranes almost linearly increased with the increase of the applied electric current. The total flux determined from the experimental data generally agreed with that determined from the simulation data.

5 Conclusion

Investigation of different mass transfer mechanisms inside ED used for regenerating liquid desiccant as lithium chloride solution was performed. ED system consisting of ten cell pairs of ion-exchange membranes was used for experimental study. Ions flus, boundary layers distribution and concentrations profile along ED membranes were numerically investigated using Nernst-Plank equation, fluid dynamic technique and COMSOL multiphysics software. The experimental results showed that the salt flux and the water flux due electro-osmosis are directly associated with applied current while the water flux due to osmosis increased with increasing the osmotic gradient along both sides of membranes. Osmosis and electro-osmosis during ED regeneration of LiCl liquid desiccant was significant and could not be neglected. On the other hand, the salt flux due osmosis was insignificant. The numerical validated simulation conducted to elucidate the relationship between concentration profile of LiCl along the membrane surface and concentration polarisation in the ED channel with respect to circulation

flow rate, applied current, and cell width. Both the experimental and the numerical results predict that concentration difference between the regenerated and spent LiCl should be minimised for an optimum ED performance.

Acknowledgements

The authors would like to thank Mr. Craig McLauchlan and Mr. John Barron for their essential help to setup the experimental tests.

References

[1] L. Pérez-Lombard, J. Ortiz, and C. Pout, "A review on buildings energy consumption information," *Energy and buildings,* vol. 40, pp. 394-398, 2008.

[2] W. Lin, Z. Ma, M. I. Sohel, and P. Cooper, "Development and evaluation of a ceiling ventilation system enhanced by solar photovoltaic thermal collectors and phase change materials," *Energy Conversion and Management,* vol. 88, pp. 218-230, 2014.

[3] Z. Duan, C. Zhan, X. Zhang, M. Mustafa, X. Zhao, B. Alimohammadisagvand*, et al.*, "Indirect evaporative cooling: Past, present and future potentials," *Renewable and Sustainable Energy Reviews,* vol. 16, pp. 6823-6850, 2012.

[4] A. J. Marszal, P. Heiselberg, J. Bourrelle, E. Musall, K. Voss, I. Sartori*, et al.*, "Zero Energy Building–A review of definitions and calculation methodologies," *Energy and Buildings,* vol. 43, pp. 971-979, 2011.

[5] K. Chua, S. Chou, W. Yang, and J. Yan, "Achieving better energy-efficient air conditioning–a review of technologies and strategies," *Applied Energy,* vol. 104, pp. 87-104, 2013.

[6] S. Wang, Z. Ma, and D.-c. Gao, "Performance enhancement of a complex chilled water system using a check valve: experimental validation," *Applied Thermal Engineering,* vol. 30, pp. 2827-2832, 2010.

[7] K. Daou, R. Wang, and Z. Xia, "Desiccant cooling air conditioning: a review," *Renewable and Sustainable Energy Reviews,* vol. 10, pp. 55-77, 2006.

[8] X. Niu, F. Xiao, and Z. Ma, "Investigation on capacity matching in liquid desiccant and heat pump hybrid air-conditioning systems," *international journal of refrigeration,* vol. 35, pp. 160-170, 2012.

[9] D. Waugaman, A. Kini, and C. Kettleborough, "A review of desiccant cooling systems," *Journal of Energy Resources Technology,* vol. 115, pp. 1-8, 1993.

[10] A. T. Mohammad, S. B. Mat, M. Sulaiman, K. Sopian, and A. A. Al-abidi, "Historical review of liquid desiccant evaporation cooling technology," *Energy and Buildings,* vol. 67, pp. 22-33, 2013.

[11] S. Misha, S. Mat, M. Ruslan, and K. Sopian, "Review of solid/liquid desiccant in the drying applications and its regeneration methods," *Renewable and Sustainable Energy Reviews,* vol. 16, pp. 4686-4707, 2012.

[12] F. A. Al-Sulaiman, P. Gandhidasan, and S. M. Zubair, "Liquid desiccant based two-stage evaporative cooling system using reverse osmosis (RO) process for regeneration," *Applied thermal engineering,* vol. 27, pp. 2449-2454, 2007.

[13] X.-W. Li and X.-S. Zhang, "Photovoltaic–electrodialysis regeneration method for liquid desiccant cooling system," *Solar Energy,* vol. 83, pp. 2195-2204, 2009.

[14] H. Strathmann, *Ion-exchange membrane separation processes* vol. 9: Elsevier, 2004.

[15] X.-W. Li, X.-S. Zhang, and S. Quan, "Single-stage and double-stage photovoltaic driven regeneration for liquid desiccant cooling system," *Applied Energy,* vol. 88, pp. 4908-4917, 2011.
[16] Q. Cheng, X.-S. Zhang, and X.-W. Li, "Performance analysis of a new desiccant pre-treatment electrodialysis regeneration system for liquid desiccant," *Energy and Buildings,* vol. 66, pp. 1-15, 2013.
[17] Y. Tanaka, "Mass transport and energy consumption in ion-exchange membrane electrodialysis of seawater," *Journal of Membrane Science,* vol. 215, pp. 265-279, 2003.
[18] V. Nikonenko, K. Lebedev, J. Manzanares, and G. Pourcelly, "Modelling the transport of carbonic acid anions through anion-exchange membranes," *Electrochimica Acta,* vol. 48, pp. 3639-3650, 2003.
[19] S. Casas, N. Bonet, C. Aladjem, J. Cortina, E. Larrotcha, and L. Cremades, "Modelling sodium chloride concentration from seawater reverse osmosis brine by electrodialysis: Preliminary results," *Solvent Extraction and Ion Exchange,* vol. 29, pp. 488-508, 2011.
[20] S. Casas, C. Aladjem, J. Cortina, E. Larrotcha, and L. Cremades, "Seawater reverse osmosis brines as a new salt source for the chlor-alkali industry: integration of NaCl concentration by electrodialysis," *Solvent Extraction and Ion Exchange,* vol. 30, pp. 322-332, 2012.
[21] M. Fidaleo and M. Moresi, "Optimal strategy to model the electrodialytic recovery of a strong electrolyte," *Journal of membrane science,* vol. 260, pp. 90-111, 2005.
[22] J. Ortiz, J. Sotoca, E. Exposito, F. Gallud, V. Garcia-Garcia, V. Montiel*, et al.*, "Brackish water desalination by electrodialysis: batch recirculation operation modeling," *Journal of Membrane Science,* vol. 252, pp. 65-75, 2005.
[23] M. Sadrzadeh, A. Kaviani, and T. Mohammadi, "Mathematical modeling of desalination by electrodialysis," *Desalination,* vol. 206, pp. 538-546, 2007.
[24] Y. Tanaka, "Irreversible thermodynamics and overall mass transport in ion-exchange membrane electrodialysis," *Journal of membrane science,* vol. 281, pp. 517-531, 2006.
[25] Z. Zourmand, F. Faridirad, N. Kasiri, and T. Mohammadi, "Mass transfer modeling of desalination through an electrodialysis cell," *Desalination,* vol. 359, pp. 41-51, 2015.
[26] Q. Cheng, Y. Xu, and X.-S. Zhang, "Experimental investigation of an electrodialysis regenerator for liquid desiccant," *Energy and Buildings,* vol. 67, pp. 419-425, 2013.
[27] Y. Guo, Z. Ma, A. Al-Jubainawi, P. Cooper, and L. D. Nghiem, "Using electrodialysis for regeneration of aqueous lithium chloride solution in liquid desiccant air conditioning systems," *Energy and Buildings,* vol. 116, pp. 285-295, 3/15/ 2016.
[28] Y. Tanaka, *Ion Exchange Membrane Electrodialysis: Fundamentals, Desalination, Separation*: Nova Science Publishers, 2010.
[29] F. Fadaei, S. Shirazian, and S. N. Ashrafizadeh, "Mass transfer modeling of ion transport through nanoporous media," *Desalination,* vol. 281, pp. 325-333, 2011.
[30] E. J. Dickinson, H. Ekström, and E. Fontes, "COMSOL Multiphysics®: Finite element software for electrochemical analysis. A mini-review," *Electrochemistry Communications,* vol. 40, pp. 71-74, 2014.
[31] K. Bawornruttanaboonya, S. Devahastin, T. Yoovidhya, and N. Chindapan, "Mathematical modeling of transport phenomena and quality changes of fish sauce undergoing electrodialysis desalination," *Journal of Food Engineering,* vol. 159, pp. 76-85, 2015.
[32] Y. Kim, "Ionic separation in electrodialysis: analyses of boundary layer, cationic partitioning, and overlimiting current," 2010.
[33] J. J. McKetta Jr, *Unit Operations Handbook: Volume 2 (In Two Volumes)* vol. 2: CRC Press, 1992.
[34] A. Selemion. (2014). Available: http://www.selemion.com/SELC.pdf

Table 1 Designed experiments for investigating the characteristics of the ED for a liquid desiccant regeneration

Cases	Description	Factors				
		C_{GT} (%)	C_{ST} (%)	$\dot{V}$ (L/h)	I (A)	Operating time (hr)
1	Osmotic pressure and water and salt diffusion	30	25	100	0	2
2		30	20	100	0	2
3		30	15	100	0	2
4		30	10	100	0	2
5		30	5	100	0	2
6	Electro-osmotic force, and salt and water mass transport	30	30	100	3 - 12	2
7		27.5	27.5	100	3 - 12	2
8		25	25	100	3 - 12	2
9		18	18	100	3 - 12	2
10	The combined effect of the variables designed using Taguchi method	29	29	60	8	1
11		29	27.5	100	10	1
12		29	26	140	12	1
13		27.5	27.5	140	10	1
14		27.5	26	60	12	1
15		27.5	24.5	100	8	1
16		26	26	100	12	1
17		26	24.5	140	8	1
18		26	23	60	10	1
19	Impact of flow rate on the ED exit concentration	27.5	27.5	60	8	2
20		27.5	27.5	100	8	2
21		27.5	27.5	140	8	2

Table 2 The parameters used in the numerical model

Parameter	Description	Value	Source
$\emptyset$	Total potential drop over unit cell (V)	1.4	Input
D_{Li}	Diffusion coefficient, Li (m^2/s)	2.31×10^{-9}	[14]
D_{Cl}	Diffusion coefficient, Cl (m^2/s)	3.11×10^{-9}	[14]
T	Temperature (K)	298.15	Input
c_G	Entrance concentration of generated channel % (wt/wt)	29.031	Input
c_S	Entrance concentration of spent channel % (wt/wt)	29.031	Input
C_{CEM}	Membrane charge concentration, Li % (wt/wt)	4	[33]
C_{AEM}	Membrane charge concentration, Cl % (wt/wt)	10	[33]
$\boldsymbol{\sigma}_{CMV}$	CMV membrane conductivity (S/m)	0.625	[28]
$\boldsymbol{\sigma}_{AMV}$	AMV membrane conductivity (S/m)	0.35	[28]
$\dot{\mathbf{V}}$	Channel average flow velocity (L/h)	60	Input
L	Cell length (m)	0.175 [m]	[34]
W_{ch}	Channel width (mm)	0.75 [mm]	[34]
W_m	Membrane width (mm)	0.18 [mm]	[34]
D_{ch}	ED cell depth (m)	0.12 [m]	[34]
$t_{w.}$	Transport number of water of electro-osmotic influence (-)	1.2	Experiment
B	Membrane water permeability due to osmotic pressure per one cell ($\frac{mol}{m^2.s.bar}$)	1.147×10^{-5}	Experiment

Table 3 Lab-scale ED system characteristics [34]

System characteristics	Value
Material of the anode plate	Ti / Ir
Material of the cathode plate	SUS316
Input Rectifier	AC 100 V * Single phase * 50/60 Hz
Output Rectifier	DC 15 V * 30 A
Storage capacity of spent, generated and Electrolyte tanks	3.5 L
ED cell depth	0.12 m
Membrane resistance	2-3 $\Omega.cm^2$
Membrane conductivity	0.6-0.9 S/m
Maximum channel average flow velocity	600 L/h
Cell length	0.175 m
ED cell depth	0.12 m
Channel width	0.75 mm
Membrane thickness	0.18 mm
Affective area of the membrane	0.021 m^2
Number of pairs of membrane	10 pairs

Table 4 Salt mass transfer within the ED under different operating conditions

Cases	C_{GT} (%)	C_{ST} (%)	$\dot{\mathbf{V}}$ (L/h)	I (A)	LiCl ($g/s.m^2$)	$\Delta\mathbf{C}$% (wt/wt)
10	29	29	60	8	0.048	0.01578
11	29	27.5	100	10	0.062	0.00847
12	29	26	140	12	0.079	0.00547
13	27.5	27.5	140	10	0.065	0.01008
14	27.5	26	60	12	0.079	0.01814
15	27.5	24.5	100	8	0.053	0.0032
16	26	26	100	12	0.082	0.01885
17	26	24.5	140	8	0.054	0.00655
18	26	23	60	10	0.071	0.01099

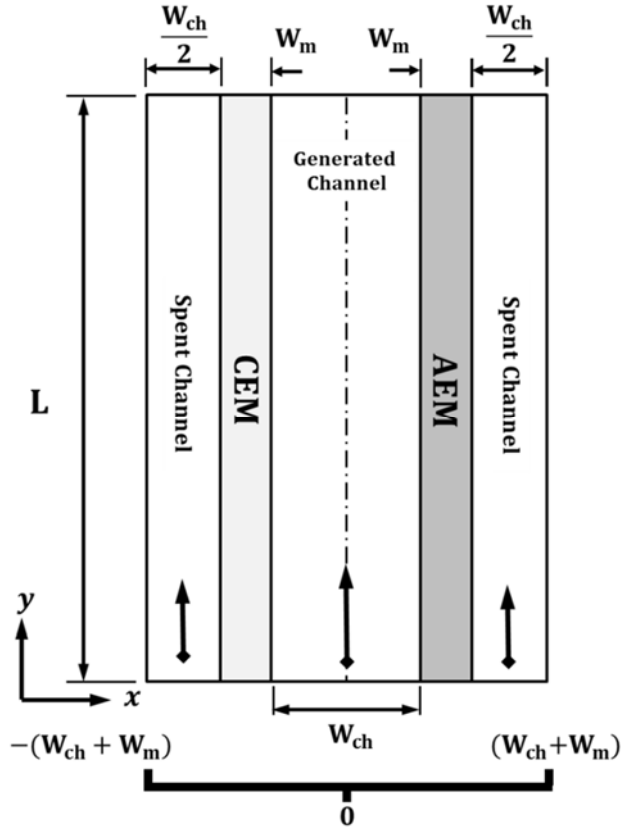

Fig. 1 Illustration of the ED model and its dimensions.

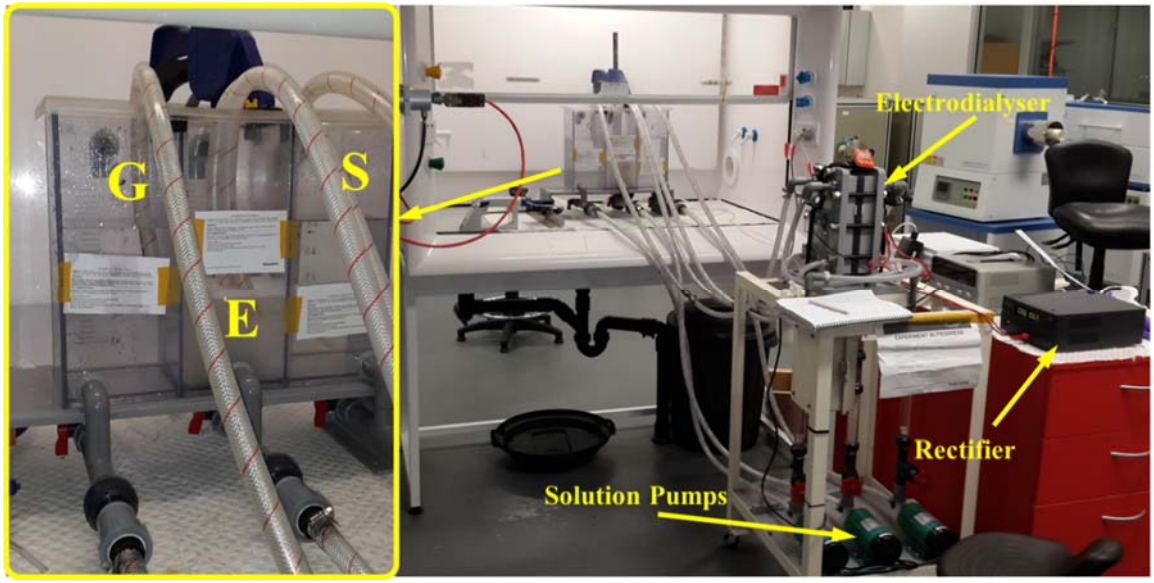

Fig. 2 Illustration of the ED experimental setup, where G, S and E represent the generated, spent and electrolyte tanks, respectively.

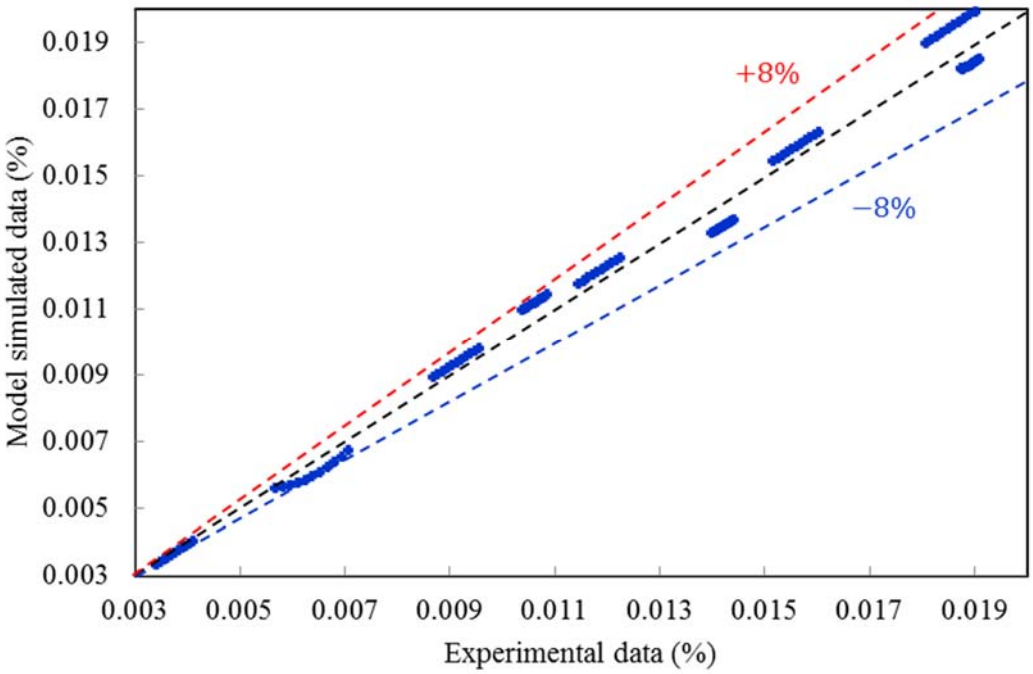

Fig. 3 Comparison between the model simulated concentration difference between the entrance and exit of the ED stack and that of derived from the experimental data.

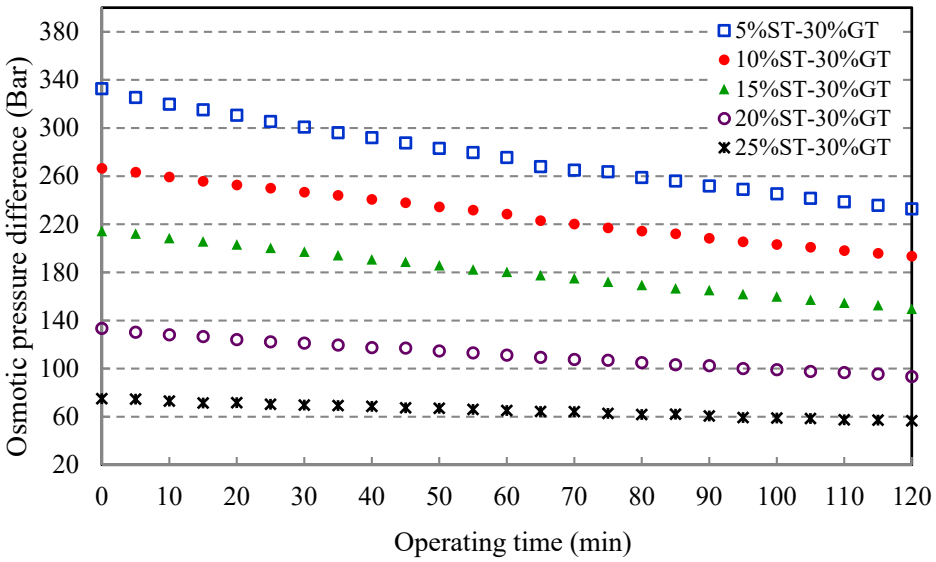

(a) Osmotic pressure difference between spent and generated channels

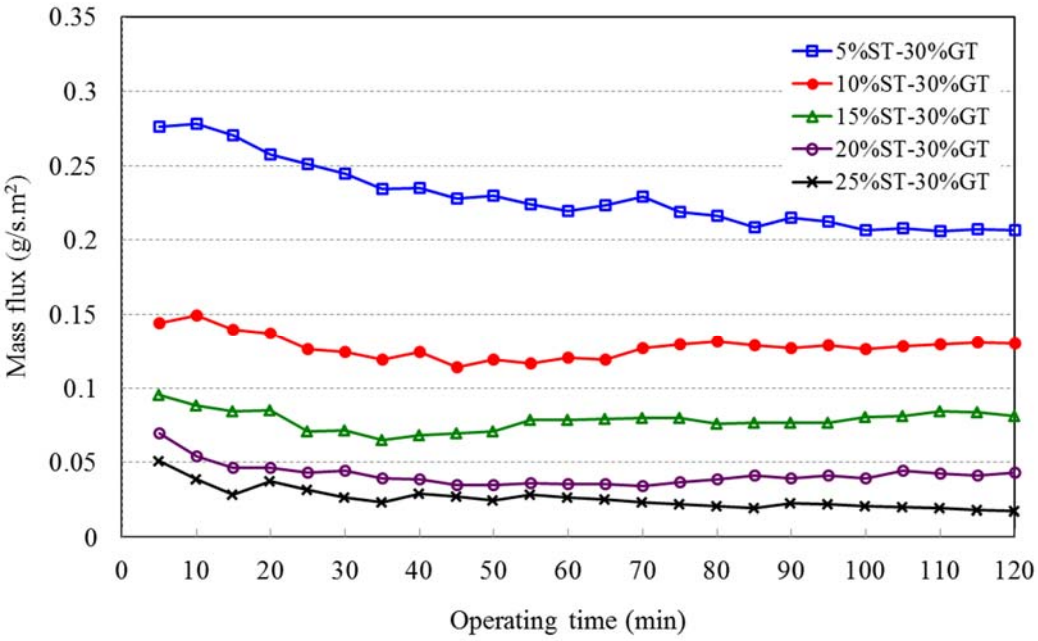

(b) Water mass transfer from the spent to generated channels

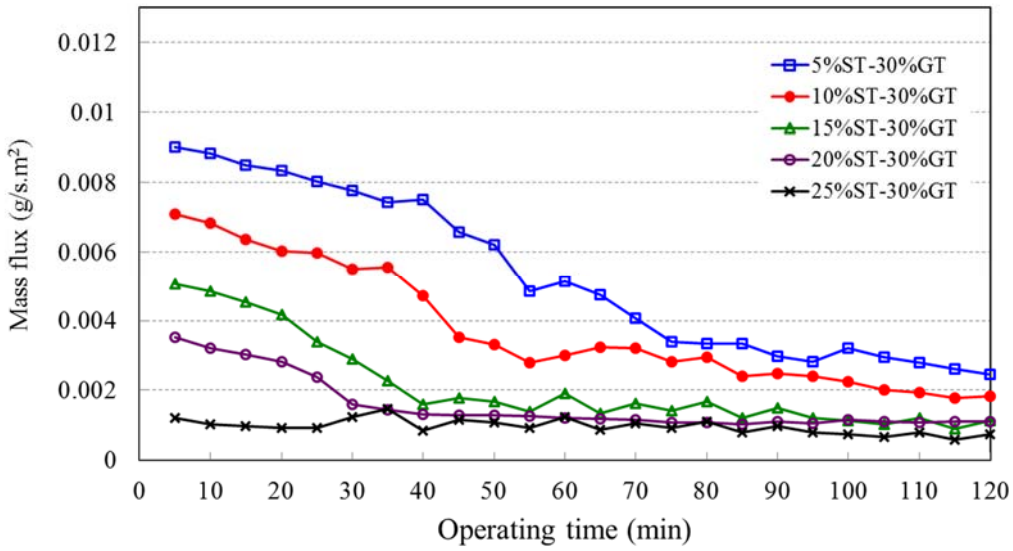

(c) Salt mass transfer from the generated to spent channels

Fig. 4 Impact of different initial solution concentrations between the spent and generated tanks on the water/salt mass transfer through the ED stack, where ST and GT represent the spent tank and generated tank, respectively.

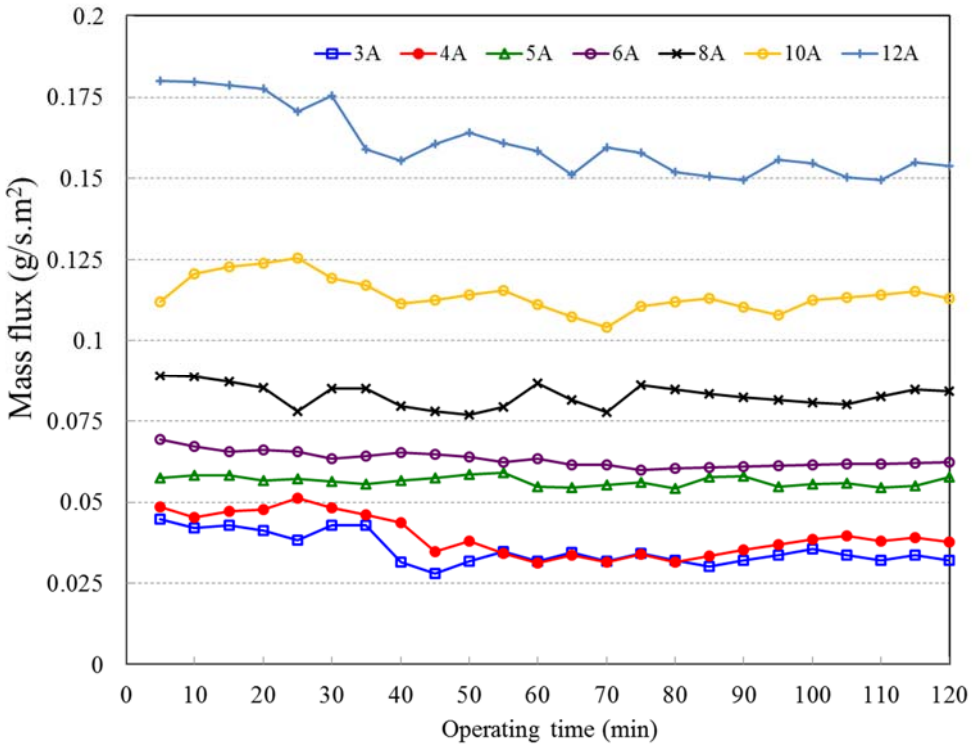

(a) $C_{GT} = 30\%$, $C_{ST} = 30\%$, and $\dot{V} = 100$ L/h

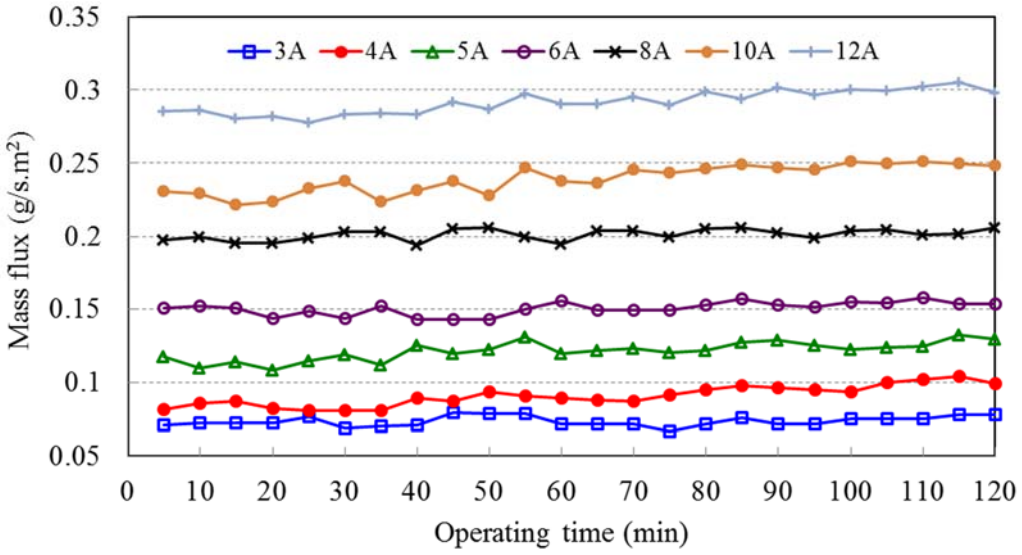

(b) $C_{GT} = 18\%$, $C_{ST} = 18\%$, and $\dot{V} = 100$ L/h

Fig. 5 Waster mass transfer from the spent to generated channels due to the impact of electro-osmosis.

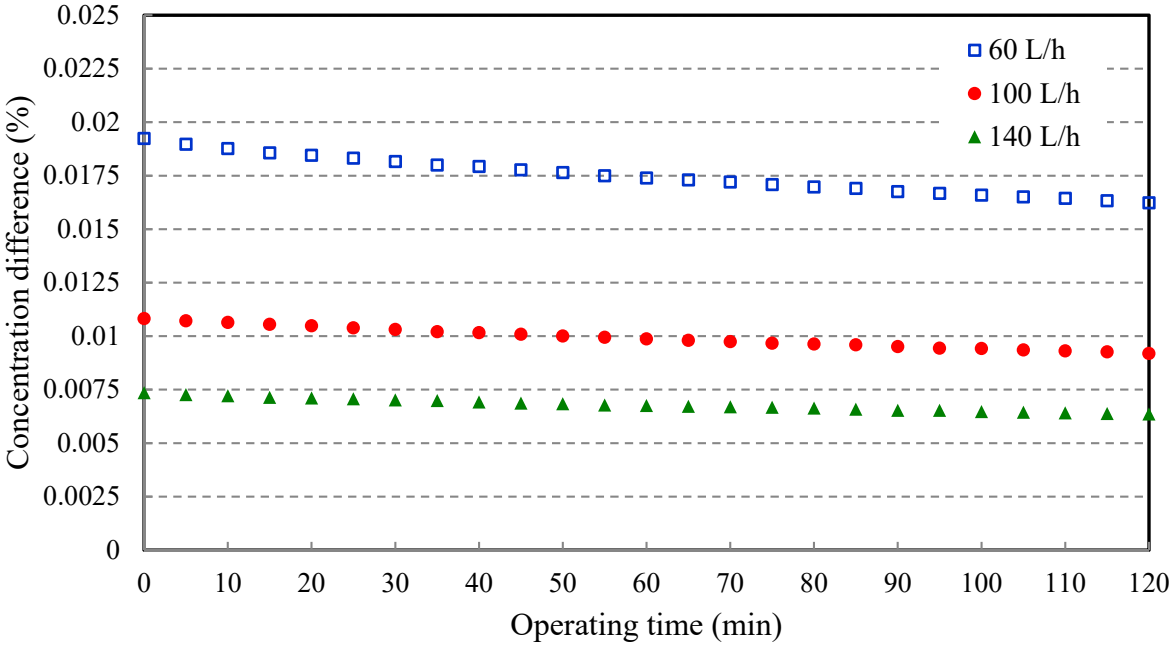

Fig. 6 Concentration difference of the generated solution between the entrance and exit of the ED stack (the initial concentrations of the solutions in both generated and spent tanks were 27.5% (wt/wt), and the applied current was 8 A).

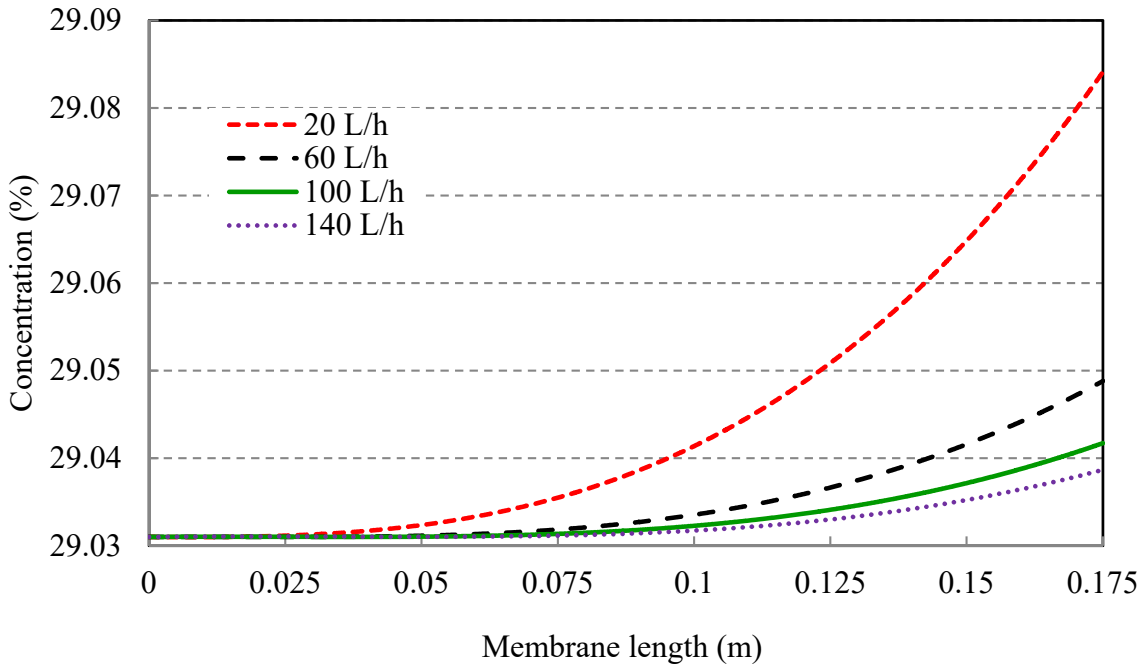

Fig. 7 Concentration of the generated solution along the membrane length under different solution flow rates.

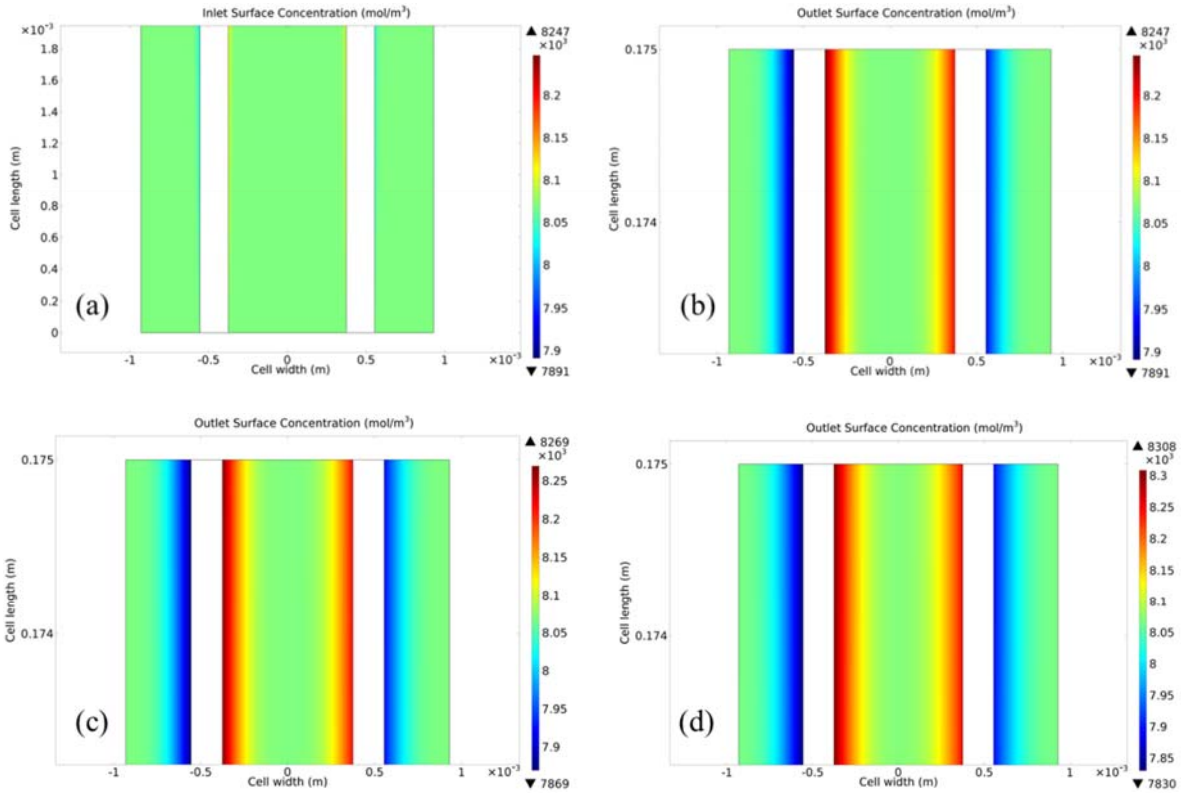

Fig. 8 Concentration distributions of the solution at the entrance and exit of the ED cell a) entrance; b) exit at 140 L/h; c) exit at 100 L/h; d) exit at 60 L/h.

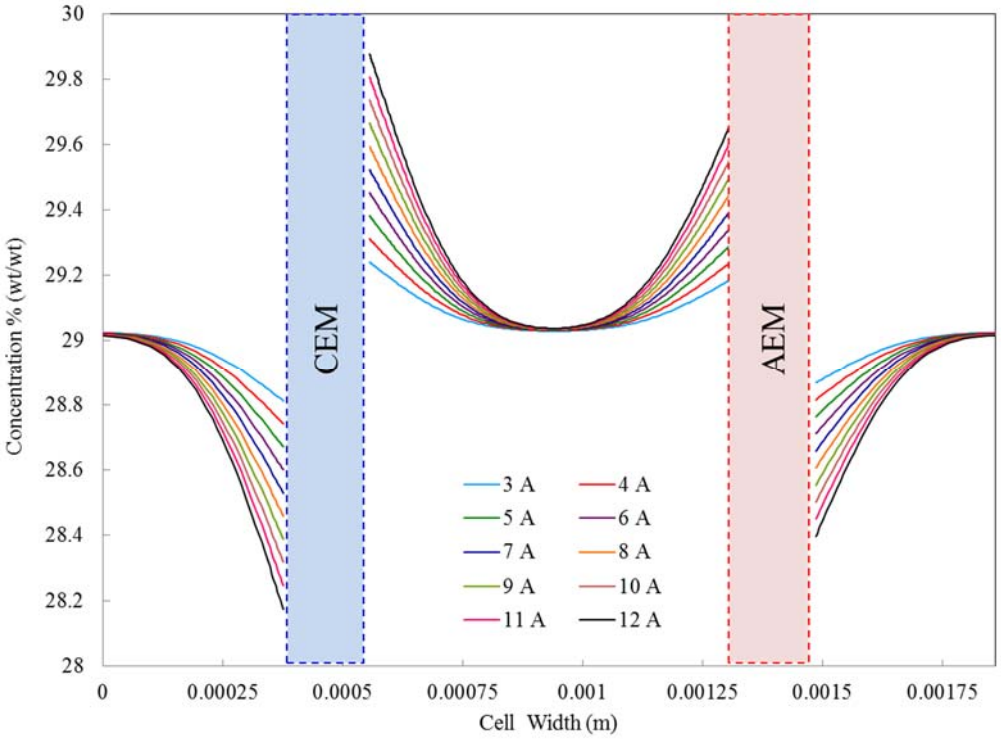

Fig. 9 Concentration distribution of the solution through the ED cell and along the membranes under different applied electrical currents.

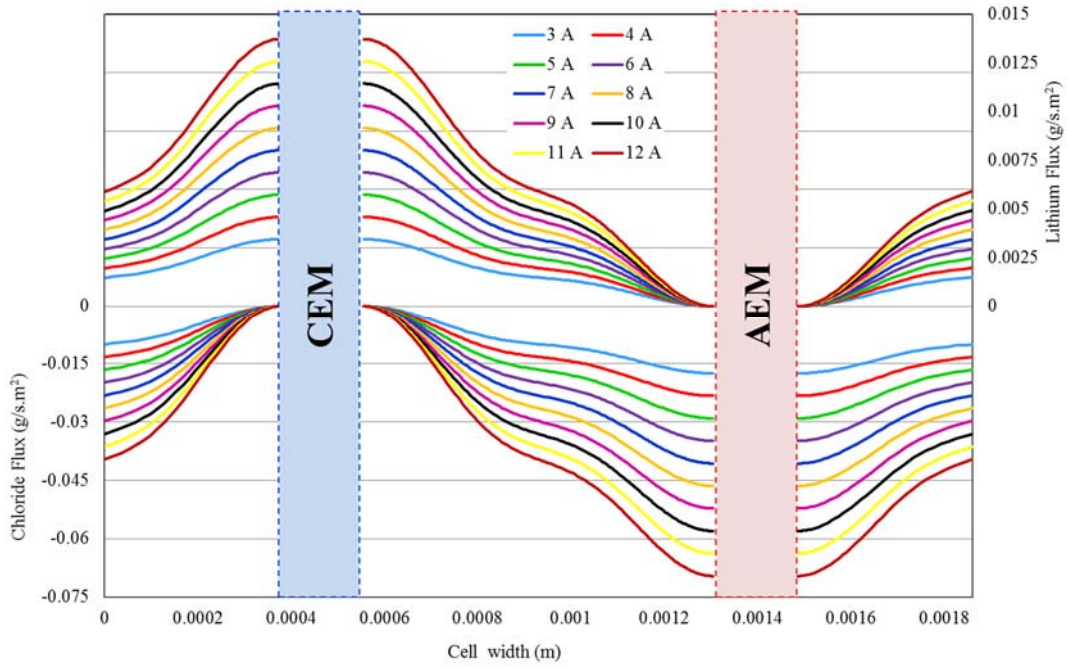

Fig. 10 Profiles of Li^+ and Cl^- fluxes along cationic and anionic membranes under different applied electric currents.

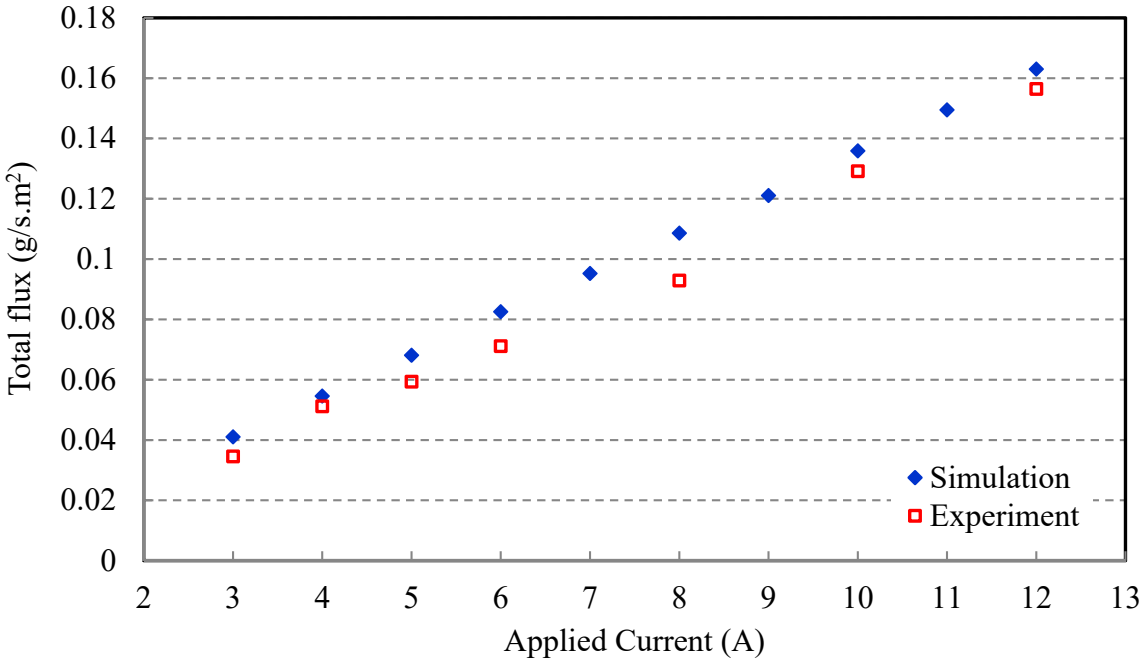

Fig. 11 Comparison of experimentally derived salt flux transferred into the generated channels with that determined from simulations.

Highlights

- The water flux due electro-osmosis are directly associated with applied current
- Due to increasing the osmotic gradient, significantly water flux increasing while the salt flux slightly increased
- Comparing the numerical simulation by the experimental results
- Investigate the variation of flow rate, applied current and inlet concentrations on different phenomenon in ED process
- The experimental and the numerical predicted that the solution flow rate and the concentration difference between the regenerated and spent LiCl solution should be minimised for an optimum ED performance